Electronic Supplementary Material (ESI) for Polymer Chemistry.

Electronic Supplementary Information

Fluorous Effect-Induced Emission of Azido Substituted Poly(vinylidene fluoride) with High Photostability and Film Formation

Zhicheng Zhang,*[a] Jie Xiong,[a] Gang He,[b] Dongfeng Dang,[a] Yunchuan Xie,[a] Qing Wang*[c]

[a] MOE Key Laboratory for Nonequilibrium Synthesis and Modulation of Condensed Matter
Xi'an Key Laboratory of Sustainable Energy Materials Chemistry
Department of Applied Chemistry, School of Science, Xi'an Jiaotong University
Xi'an, Shaanxi Province, P. R. China, 710049
E-mail: zhichengzhang@mail.xjtu.edu.cn

[b] Frontier Institute of Science and Technology, Xi'an Jiaotong University
Xi'an, Shaanxi Province, P. R. China, 710054

[c] Department of Materials Science and Engineering
The Pennsylvania State University, University Park
Pennsylvania, USA, 16802
E-mail: wang@matse.psu.edu

1. Experimental section

Reagents and Materials: Poly(vinylidene fluoride-chlorotrifluoroethylene)s (P(VDF-CTFE)s) with 6, 9, and 20 mol% CTFE and average molecular weight (M_w) of 200,000 were provided by China Bluestar Chengrand Chemical Co. Ltd., Polyvinyl chloride (PVC, Sigma-Aldrich), sodium azide (NaN_3, Sigma-Aldrich, ⩾99.5%), sodium chloride (NaCl, Tianjin Reagents Co. Ltd., AR grade), *N,N*-dimethylformamide (DMF, Tianjin Reagents Co. Ltd., AR grade), tetrahydrofuran (THF, Tianjin Reagents Co. Ltd., AR grade), *N*-methylpyrrolidinone (NMP, Tianjin Reagents Co. Ltd., AR grade), and acetone (Tianjin Reagents Co. Ltd. AR grade) were commercially available and used as received without further purification.

Analytical Methods: ^1H and ^{19}F NMR spectra were obtained from a Bruker (Advance III) 400 MHz spectrometer with acetone-d_6 as solvent and tetramethylsilane (TMS) as an internal standard. Fourier transform infrared (FTIR) was performed on a Tensor 27 FTIR spectrometer (Bruker Corporation, Germany). UV-Vis spectra was recorded with a Shimadzu UV-2250 spectrophotometer at ambient temperature. Emission spectra and photo-bleaching measurements were carried out at room temperature on a Hitachi F-4500 fluorescence spectrophotometer. The mechanical properties of the fluoropolymer films were tested with a material testing machine (CMT 6503 produced by Shenzhen Suns Technology Stock Co. Ltd.) at a tensile speed of 200 mm min^{-1}. The samples were cut into dumbbell shapes (the testing part with a width of 10 mm and a thickness of about 0.15 mm). The luminescent images were taken on an Olympus BX53 (Olympus Corporation) at UV, blue, and green light

excitations onto slide glasses. Differential scanning calorimetric (DSC) analysis was conducted on a Netzsch DSC 214 Polyma DSC21400A-0466-L (Netzsch, Germany) under a nitrogen atmosphere at a scanning rate of 10 °C min^{-1}. Thermogravimetric analysis (TGA) was performed on a NETZSCH TG 209C (NETZSCH Corporation, Germany) thermogravimetric analyser. 3-5 mg of the sample were placed in a platinum pan and were heated under a nitrogen atmosphere from 30 to 700 °C, at a heating rate of 10 °C min^{-1}. Molecular weight was determined by gel permeation chromatography (GPC) measurements were performed in DMF with an elution rate of 0.5 mL/min on a TOSOH equipped with a Bryce refractive index detector. Two columns were employed, including one 4 μm superAW2500 gel column and one 4 μm superAW3000 columns.

Synthesis of azido substituted PVDF [P(VDF-ATrFE)]: The synthesis of fluoropolymer containing azido groups is conducted in the following procedure. P(VDF-CTFE) (94/6, 2.00 g) and DMF (60 mL) were introduced into a three-neck round-bottomed flask equipped with a magnetic stirrer. The temperature was maintained at 55 °C for 1 h until the polymer was completely dissolved. NaN_3 (0.36 g) was carefully added into the flask and the mixture was stirred at 55 °C for 20 h. The resultant copolymer was obtained by precipitating the reaction mixture into saturated NaCl aqueous solution. The precipitant was washed with deionized water to remove the residual reagent and NaCl, and then dried at 50 °C under reduced pressure for 24 h. P(VDF-CTFE) (91/9) and P(VDF-CTFE) (80/20) were reacted with 0.53 and 0.60 g of NaN_3 respectively to yield the corresponding P(VDF-ATrFE)s following the same

procedure under the identical conditions. ^{1}H and ^{19}F NMR were applied to determine the exact chemical composition of the resultant copolymers. The copolymers prepared from P(VDF-CTFE) with VDF/CTFE = 94/6, 91/9, 80/20 in mol% were termed as P(VDF-ATrFE)-6, P(VDF-ATrFE)-9, and P(VDF-ATrFE)-20, respectively. NMR results indicate that over 95 mol% of C-Cl bonds of CTFE have been successfully transformed into azido groups.

Synthesis of azido substituted PVC copolymers [P(VC-VAz)]: The azido substitution of PVC was conducted for comparison purpose in the following procedure. PVC (2.00 g) and DMF (60 mL) were placed into a round-bottomed flask equipped with a magnetic stirrer. The temperature was maintained at 60 ^{o}C for 2 h until the polymer was completely dissolved. NaN_3 (1.00 g) was carefully introduced into the solution followed by continuous stirring for another 8 h at 60 ^{o}C. The resultant copolymer was obtained by precipitating the reaction mixture into deionized water, following by washing the precipitant with deionized water three times to remove the residual salt. The resultant solid was dried at 50 ^{o}C under reduced pressure for 24 h. The content of resultant copolymer was determined with ^{1}H NMR and further characterized with FTIR.

Fabrication of films: All the films were fabricated via a solution cast process in the following procedure. The fine copolymer solution (about 3 wt% in DMF) was cast onto glass plates. After the solvent was evaporated completely at 50 ^{o}C, the as-formed copolymer films were peeled off from glass plates and dried at ambient temperature in vacuum for 24 h before measurement.

Nanofibers prepared from electrospinning process: P(VDF-ATrFE)-6 solution (0.11 g in 5 mL of acetone) was used for electrospinning to prepare nanofibers. An injector with a steel syringe needle connecting to the high-voltage supply was filled with the P(VDF-ATrFE)-6/acetone solution. Glass slides put on an Al sheet connected to the ground were used for the samples collection. The distance between the syringe needle and receiver was fixed at 15 cm and the voltage was fixed at 15 kV.

Measurement of AIE behavior of ASFPs: To confirm the AIE performance of P(VDF-ATrFE) copolymers, their fluorescence emission behavior was investigated in DMF and DMF/ethanol mixtures, where DMF was serving as the good solvent and ethanol was the nonsolvent. The concentration was well maintained as a constant of 0.45 mg mL^{-1} for all the solutions, where the ethanol content is increased from 0 to 90 vol% with a step of 10 vol%. The fluorescent results were obtained under 320 nm emission light.

Quantum Yield of the P(VDF-ATrFE): The solution quantum yield values were calculated corresponding to the following equation:

$$\Phi_u = \frac{\Phi_s Y_u A_s n_u^2}{Y_s A_u n_s^2}$$

where Φ is the quantum yield, Y is the measured integrated fluorescence emission intensity, A is the optical density measured at the excitation wavelength, and n is the refractive index of the solvent. The subscript "*s*" refers to the standard quantum yield of reference quinine sulfate (quantum yield = 54% in 0.1 M H_2SO_4). The subscript "*u*" refers to the unknown quantum yield of P(VDF-ATrFE)s. In order to minimize the reabsorption effect, absorbance in the 1 cm fluorescence cuvette were kept under

0.05. The quantum yield of the films was determined using an integrating sphere.

2. Further Characterization of P(VDF-ATrFE)s and P(VC-VAz)

The successful substitution of azido groups onto P(VDF-CTFE)s could be further confirmed with ^{19}F NMR results. ^{19}F NMR spectra of P(VDF-CTFE) and the resultant copolymers are compared in Fig. S1(a), and the assignment of all the signals are summarized in Table S1. The resonances at -92.3 ppm (signal b), -94.0 to -96.2 ppm (signal e), -114.7 ppm (signal k), and -117.0 ppm (signal l) are assigned to VDF connected with VDF in the sequence of -$CF_2CH_2C\boldsymbol{F_2}CH_2CF_2$-, -$CH_2CH_2C\boldsymbol{F_2}CH_2CF_2$, -$CF_2CH_2C\boldsymbol{F_2}CF_2CH_2$-, and -$CH_2CF_2C\boldsymbol{F_2}CH_2CH_2$-, respectively. The substitution of Cl atoms with azido groups causes invisible change in these signals. The signals obtained at -92.6 to -94.4 ppm (signal c), -109.1 ppm (signal g), -109.3 to -110.8 ppm (signal h), -118.2 to -120.4 ppm (signal m), and -120.4 to -123.3 ppm (signal n) are corresponding to CTFEs and adjacent VDF units in the sequences of -$CFClCH_2C\boldsymbol{F_2}CH_2CF_2$-, -$CF_2CH_2C\boldsymbol{F_2}CF_2CFCl$-, -$CF_2CFClC\boldsymbol{F_2}CFClCH_2$-, -$CH_2CF_2C\boldsymbol{F_2}CFClCH_2$-), and -$CF_2CF_2C\boldsymbol{F}ClCH_2CF_2$- in pristine P(VDF-CTFE)s. After reacted with NaN_3, these signals are completely eliminated in the target product P(VDF-ATrFE), which indicates all the CTFEs in pristine P(VDF-CTFE) are involved in the reaction. The new resonance signals appeared at -92.7 to -93.8 ppm (signal d) and -108.2 ppm (signal f) are attributed to -$CFN_3CH_2C\boldsymbol{F_2}CH_2CF_2$- and -$C\boldsymbol{F_2}CFN_3CH_2CF_2$- sequences, which could confirm the successful substitution of -Cl by -N_3. Besides of the substitution reaction, a small portion of CTFE adjacent to VDF in -CF_2CFCl-CH_2CF_2- would undergo a dehydrochlorination catalyzed by the basic

NaN_3 involving the removal of one molecular HCl and the formation of -CF_2CF=$CHCF_2$- structure. That could be confirmed by the signals generated at -89.2 ppm (peak a, -CF=CHC***F***$_2CH_2CF_2$-), -110.1 to -111.4 ppm (peak i, -CF_2CFClC***F***$_2$CF=CH-), -113.4 and -113.7 ppm (peak j, -CF_2CF_2C***F***=$CHCF_2$- and -CH_2C***F***$_2CF_2CF$=CH-) on ^{19}F NMR of the resultant P(VDF-ATrFE)s.

The substitution and elimination reactions could be further confirmed by the FTIR results of pristine P(VDF-CTFE) and resultant P(VDF-ATrFE)-6 as shown in Fig. S1(b). The characteristic asymmetric azido stretch peak emerging at 2147 cm^{-1} in the P(VDF-ATrFE) may address for the existence of -N_3 groups. The new bands appearing at 3434 cm^{-1} and 1652 cm^{-1} corresponding to the stretching vibration of =C-H and C=C, respectively, which are related to the -CF=CH- bonds generated from dehydrochlorination reaction of -CFCl-CH_2- units.

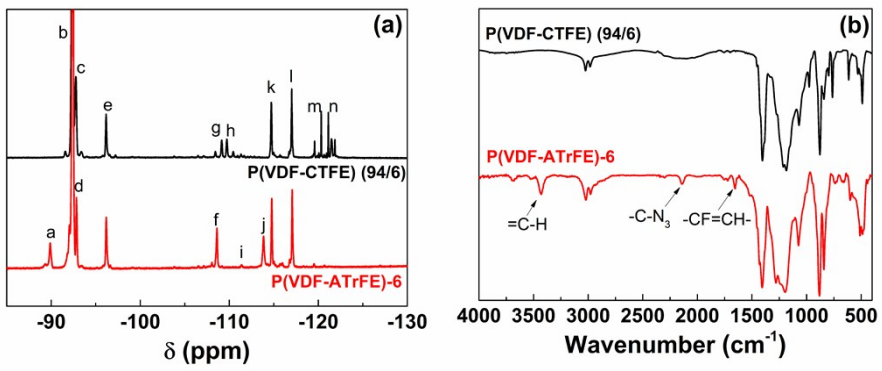

Fig. S1. (a) ^{19}F NMR (acetone-d_6) and (b) FTIR spectra of P(VDF-CTFE) (94/6) and P(VDF-ATrFE)-6.

Table S1 ^{19}F NMR chemical shifts and assignments of P(VDF-CTFE) and P(VDF-ATrFE)-6.

Peaks	Structure	Chemical shift (ppm)
a	-CF=CHC***F*****2**CH_2CF_2-	-89.2
b	-CF_2CH_2C***F*****2**CH_2CF_2-	-92.3
c	-$CFClCH_2C$***F*****2**CH_2CF_2-	-92.6 to -94.4
d	-CFN_3CH_2C***F*****2**CH_2CF_2-	-92.7 to -93.8
e	-CH_2CH_2C***F*****2**CH_2CF_2	-94.0 to -96.2
f	-***C F*****2**$CFN_3CH_2CF_2$-	-108.2
g	-CF_2CH_2C***F*****2**CF_2CFCl-	-109.1
h	-CF_2CFClC***F*****2**$CFClCH_2$-	-109.3 to -110.8
i	-CF_2CFClC***F*****2**CF=CH-	-110.1 to -111.4
j	-CF_2CF_2C***F***=$CHCF_2$-, -CF_2CH_2C***F*****2**CF_2CF=CH-	-113.4, -113.7
k	-CF_2CH_2C***F*****2**CF_2CH_2-	-114.7
l	-CH_2CF_2C***F*****2**CH_2CH_2-	-117.0
m	-CH_2CF_2C***F*****2**$CFClCH_2$-	-118.2 to -120.4
n	-CF_2CF_2C***F***$ClCH_2CF_2$-	-120.4 to -123.3

For comparison purpose, PVC is reacted with NaN_3 as well to synthesize P(VC-VAz) following the similar procedure in DMF. The chemical structure and composition of the objective P(VC-VAz) are well characterized with ^{1}H NMR and FTIR as presented in Fig. S2. About 24 mol% Cl atoms onto VC (-CH_2CHCl-) units are substituted and turned into VAz (-CH_2CHN_3-) structure. Besides substitution reaction, about 0.8 mol% VC is involved into the dehydrochlorination reaction to form -CH=CH- units as well.

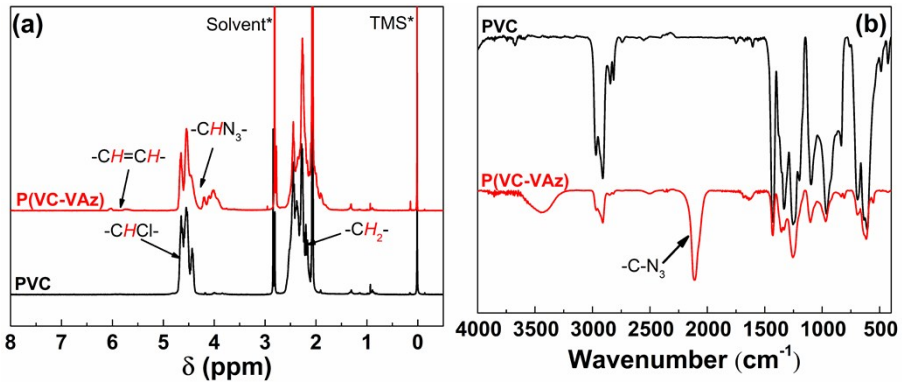

Fig. S2. (a) ^{1}H NMR and (b) FTIR of PVC and P(VC-VAz).

3. Effect of aggregation onto the emission intensity

To examine the AIE or CTE performance of ASFPs, the solutions in DMF/ethanol mixtures are exposed to UV light with 320 nm wavelength. As shown in Fig. S3a, as the content of none-solvent ethanol increases from 0 to 90 vol%, invisible fluorescence intensities could be detected with respect to the measurement error. According to the previous reports,[1,2] as for AIE or CTE active molecules, the fluorescence intensity would show a sudden increase with the increasing of the poor solvent. However, the independent fluorescence intensity of ASFPs against the solubility of the solvents strongly suggest that P(VDF-ATrFE) copolymers should be excluded from AIE or CTE-active. The slight red shift (ca. 5 nm) of the maximum emission might be attributed to the polarity change of the solution induced by the introduction of ethanol.[3] For comparison purpose, AIE performance of P(VC-VAz) has been examined as well. As shown in Fig. S3b, the emission intensity of P(VC-VAz) in DMF/ethanol mixtures with increased ethanol content is slightly change as well. Apparently, both copolymers are rather different from either AIE or CTE active molecules.

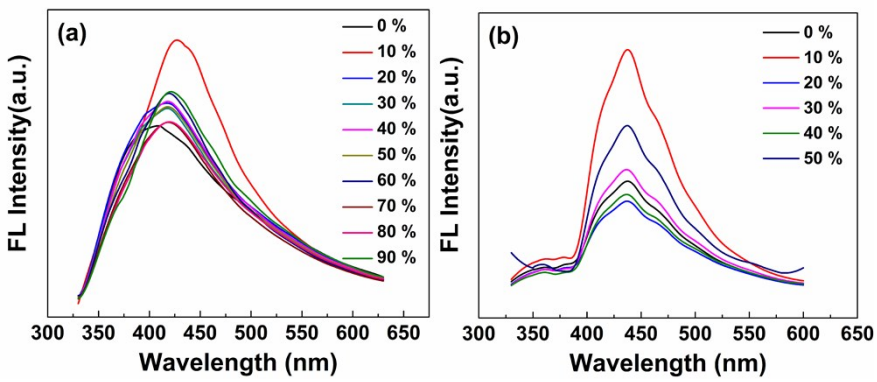

Fig. S3. Emission spectra of (a) P(VDF-ATrFE)-6 and (b) P(VC-VAz) in DMF/ethanol mixtures (0.45 mg mL^{-1}) with different f_w of ethanol under 320 nm excitation light.

4. Absorption behaviours in solutions

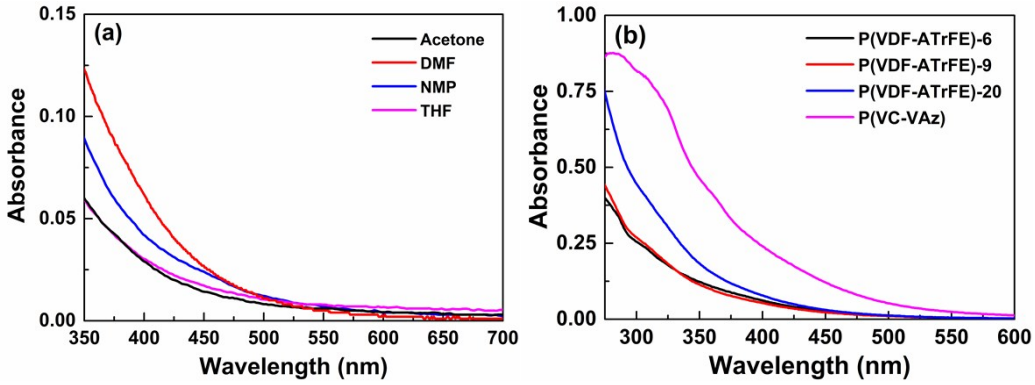

Fig. S4. (a) Absorbance of P(VDF-ATrFE)-6 dissolved in various solvents (acetone, DMF, NMP, and THF) with a concentration of 2 mg mL^{-1} (b) UV-Vis absorption of P(VC-VAc) with 24 mol% VAz and P(VDF-ATrFE)s synthesized from P(VDF-CTFE) precursors bearing 6, 9, 20 mol% CTFE in DMF solutions with concentration of 2 mg mL^{-1}.

5. Fluorescence decay process of P(VDF-ATrFE)s

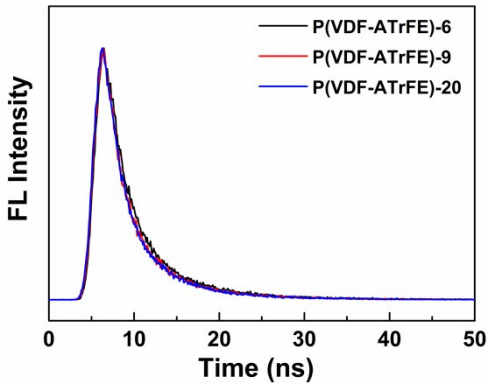

Fig. S5. Fluorescence decay curves (350 nm excitation, and monitored through 430 nm bandpass filter) of P(VDF-ATrFE)s in DMF solution.

6. Surface and mechanical properties of P(VDF-ATrFE)s.

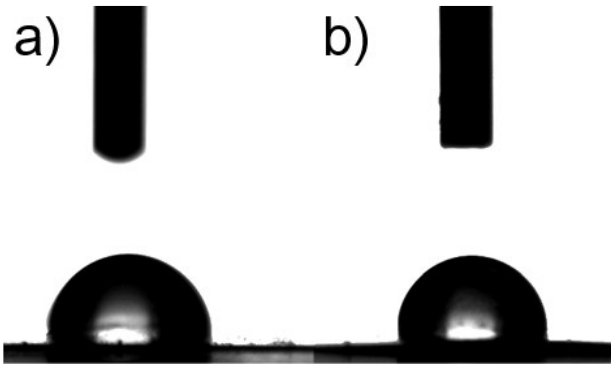

Fig. S6. Image of (a) water (with water contact angle (CA) of 94 ± 0.3°) and (b) n-hexane droplet (with n-hexane contact angle (CA) of 94 ± 0.4°) sitting on the hydrophobic and lipophobic P(VDF-ATrFE)-6 film.

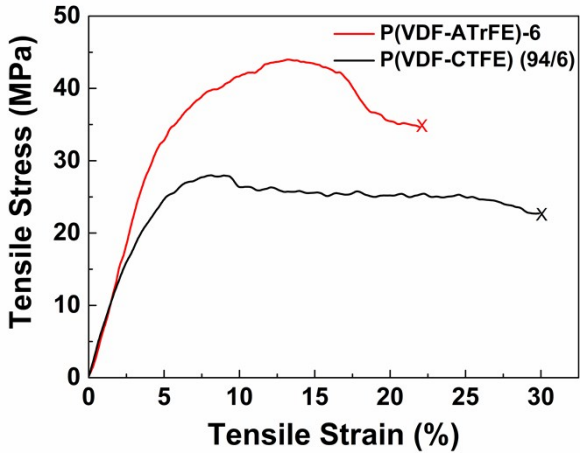

Fig. S7. Stress-strain curves of the P(VDF-CTFE) (94/6) and P(VDF-ATrFE)-6 films.

Table S2. Mechanical properties of the P(VDF-co-CTFE) and P(VDF-ATrFE)-6 films.

Films	Tensile stress (MPa)	Elongation at break (%)	Tensile modulus (MPa)
P(VDF-CTFE) (94/6)	25.2 ± 2.4	26.3 ± 7.5	352.3 ± 75.4
P(VDF-ATrFE)-6	41.8 ± 4.3	17.6 ± 7.9	727.2± 62.0

7. Thermal properties of the resultant polymers

As shown in Fig. S8 (a), a significant exothermic peak in DSC curves are observed at 130 and 145 °C in P(VDF-ATrFE)-20 and P(VC-VAz) correlated to the decomposition of azido group. In addition, as shown in Fig. S8 (b), the thermal weight loss of P(VDF-ATrFE)-20 is observed at 110-200 °C, which could be attributed to the decomposition of azido group as well. Due to the relatively low content of azido group in P(VDF-ATrFE)-6 and 9, the decomposition of azido groups could hardly be detected from DSC and TGA. However, the truth that heating the bulky polymer at over 100 °C may cause the crosslinking of P(VDF-ATrFE)-6 and 9 may confirm the decomposition of azido groups as well. Therefore, owing to the decomposition of azido groups, P(VDF-ATrFE)s and P(VC-VAz) could only be stably stored and operated below 100 °C.

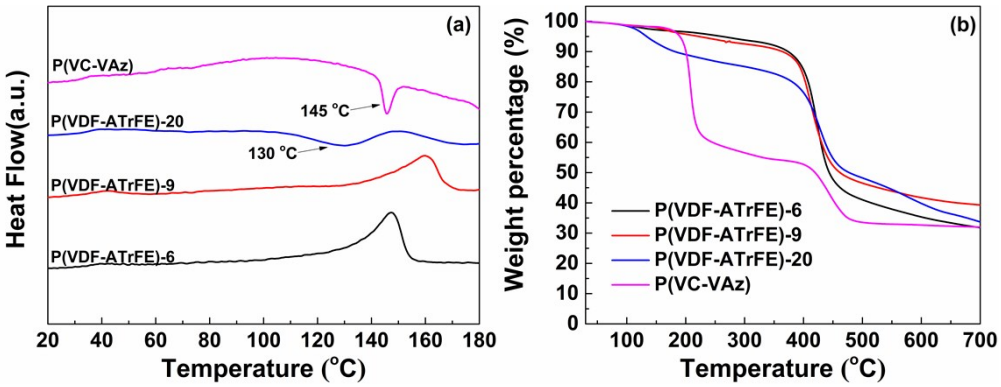

Fig. S8. (a) Differential scanning calorimetry thermograms and (b) thermal gravimetric analysis under nitrogen atmosphere of P(VDF-ATrFE)s and P(VC-VAz).

8. Molecular weight of the resultant polymers

According to the GPC results (Fig. S9), compared to the P(VDF-CTFE)s and PVC, the molecular weight of result copolymers P(VDF-ATrFE)s and P(VC-VAz) are well maintained, which means there is no significant main chain scission.

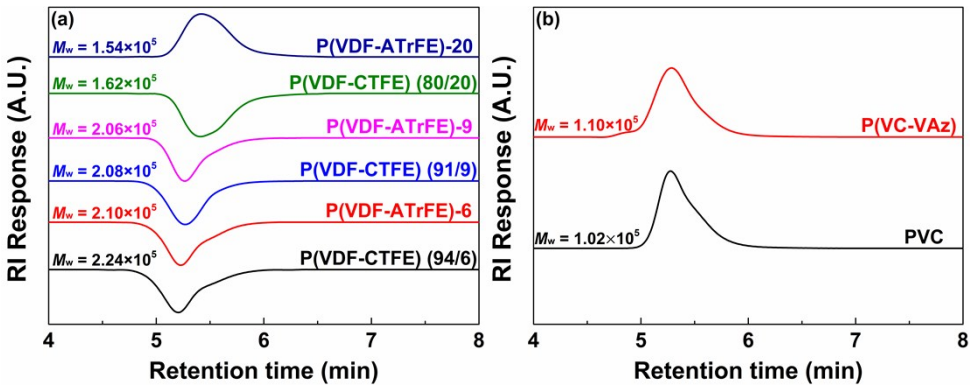

Fig. S9. GPC of (a) P(VDF-ATrFE)s and (b) P(VC-VAz).

References

1. H. Q. Deng, T. Han, E. G. Zhao, R. T. K. Kwok, J. W. Y. Lam and B. Z. Tang, *Macromolecules*, 2016, **49**, 5475-5483.

2. Y. W. Wu, B. Z. He, C. Y. Quan, C. Zheng, H. Q. Deng, R. R. Hu, Z. J. Zhao, F. Huang, A. J. Qin and B. Z. Tang, *Macromol. Rapid Commun.*, 2017, **38**, 1700070.

3. Z. X. Zhou, X. Z. Yan, M. L. Saha, M. M. Zhang, M. Wang, X. P. Li and P. J. Stang, *J. Am. Chem. Soc.*, 2016, **138**, 13131-13134.